JOURNAL OF Applied Polymer SCIENCE

Synthesis and Characterization of Nanoclay–Polymer Composites from Soil Clay with Respect to Their Water-Holding Capacities and Nutrient-Release Behavior

Subhas Sarkar, Samar Chandra Datta, Dipak Ranjan Biswas
Division of Soil Science and Agricultural Chemistry, Indian Agricultural Research Institute, New Delhi 110012, India
Correspondence to: S. C. Datta (E-mail: samar1953@yahoo.com)

ABSTRACT: Water and nutrients are two important inputs to agriculture that need to be used judiciously with higher efficiency to save these limited resources. For these purposes, a series of nanoclay–polymer composite (NCPC) superabsorbent nutrient carriers were prepared. These NCPCs were based on the reactions of different types of nanoclays (10 wt %) with partially neutralized acrylic acid and acryl amide by a free-radical aqueous solution copolymerization reaction with *N,N′*-methylene bisacrylamide as a crosslinker and ammonium persulfate as an initiator. The nanoclays isolated from three different types of soils were dominant in kaolinite (clay **I**), mica (clay **II**), and montmorillonite (clay **III**), and a portion of each was freed from amorphous aluminosilicate. Thus, there were six different types of nanoclays used, namely, those dominated by kaolinite, mica, and smectite with and without amorphous aluminosilicate. Fourier transform infrared spectroscopy and X-ray diffraction (XRD) investigations showed evidence of interaction between the clays and polymer. XRD investigation also showed that the reaction between the polymer and clays **I** and **II** occurred on the surface of various clay particles without intercalating into the stacked silicate galleries, whereas in the case of clay **III** (the smectite-dominated clay), evidence indicated the intercalation of polymer into the stacked silicate galleries of the clay and the exfoliation of the clay. The water absorbency decreased in the NCPCs compared to that of the pure polymeric hydrogel. In case of the pure polymer, the entire amount of nutrient loading released within 15 h of incubation; this was higher than that of the NCPCs. In the initial stage (up to 15 h), no significant differences in nutrient release were observed among the different polymer/clay composites, but there were differences in later stages. Among the different NCPCs, the percentage release of nutrients at 48 h ranged from around 70% in the polymer/clay **III** composite to 90% in the polymer/clay **I** composite. The presence of amorphous aluminosilicates in clay did not make any difference in the nutrient-release rate. © 2013 Wiley Periodicals, Inc. J. Appl. Polym. Sci. **2014**, *131*, 39951.

KEYWORDS: clay; hydrophilic polymers; properties and characterization

Received 26 February 2013; accepted 9 September 2013
DOI: 10.1002/app.39951

INTRODUCTION

Water and nutrients are the two important inputs in agriculture that have to be used judiciously with higher efficiency to save these limited resources. Among nitrogen (N) fertilizers, the most widely used one is urea because of its high N content (46%) and comparatively low cost of production. However, because of surface runoff, leaching, and volatilization, the utilization efficiency or plant uptake of urea is about 30–40%[1] and that of phosphorus (P) fertilizer is about 15–25%.[2] These low efficiencies cause large economic and resource losses. The loss of urea could cause very serious environmental problems.[3] Loss of N to the environment usually takes place when high concentrations of soluble N forms are present in the soil solution in excess compared to the amount that plants can take up. On the other hand, it is well known that water-soluble P is converted to water-insoluble P after reaction with soil minerals; this results in a decrease of P availability. In general, the reactions are concentration dependent. This implies that one single application of highly soluble P is likely to result in a rapid reduction of available forms; several terms, including *phosphorus sorption, adsorption, retention, fixation, precipitation,* and *immobilization,* have been used to describe these processes. Fertilizer regimes could benefit greatly from more effective time-release mechanisms, which can increase nutrient use efficiency by reducing nutrient losses, and can prevent surface and ground-water pollution. One method of effectively reducing nutrient losses is the use of slow- or controlled release fertilizers.

Superabsorbents are three-dimensionally crosslinked hydrophilic polymers that are water insoluble, hydrogel forming, and capable of absorbing large amounts of aqueous fluids. They can be

used in agriculture to improve soil moisture retention capacity; thus, the germination of seeds and plant growth can be promoted.[4] However, their application in the field has faced some problems because most of these traditional superabsorbents are based on pure polymer (sodium acrylate), have poor physical strength, and are not suitable for saline-containing water and soils.[5] When nutrients are loaded into a hydrogel, they are released quickly with high permeability. So, research on the preparation of supersorbent materials with good physical strength and nutrient-holding capacities was initiated. Among the various methods used, the introduction of inorganic clay, such as kaolin,[6] montmorillonite,[7,8] Attapulgite,[9] mica,[10] bentonite, or sercite,[11] into a pure polymeric network is a good method for reducing production costs and improving the swelling properties and hydrogel strengths. Moreover, it was found that the incorporation of kaolin nanopowder into a superabsorbent polymer can decrease the diffusion coefficient of urea release from urea-loaded composite hydrogels.[12] In general, the large specific surface area and small average particle size of clay favor even dispersion in a solvent and reactions with a given polymer.[10] However, most of these studies reported the effect of the introduction of pure crystalline clay and not soil clay, which contains noncrystalline clay also, on the improvement of water absorbency, thermal stability, gel strength, and so on, and little information is available on the effect of incorporated clay and the types of clay on the release behavior of nutrients from nutrient-loaded superabsorbent composites. In fact, this is critically important for researchers to choose specific types of clay to obtain an optimum combination of water absorbency and slow release of nutrients from clay–polymer composites.

With this background and to explore the possibility of using these high-surface-area nanomaterials, this investigation was carried out with the following objectives:

1. To synthesize clay–polymer–nutrient nanocomposites with crystalline and noncrystalline components of soil clays.
2. To characterize the nanocomposite materials by different physical and chemical methods.
3. To test the nanocomposite materials in terms of N and P release behavior.

EXPERIMENTAL

Materials

Urea and diammonium phosphate (DAP) granule fertilizer were laboratory chemicals; and the others were all analytical grade. Acrylic acid (AA), acrylamide (Am), *N,N′*-methylene bisacrylamide, and ammonium persulfate were purchased from Loba Chemicals. All of the chemicals used were available from commercial sources.

Separation of the Nanoclay from Soil

The nanosized clays were separated from three different soils, namely, soils dominated by kaolinite (clay **I;** Alfisol), mica (clay **II;** Inceptisol), and smectite (clay **III;** Vertisol). Soil samples of about 100 g were taken from each soil order for clay separation and fractionation. Calcium carbonate, organic matter, and iron–aluminum oxides were removed from all three soil samples.[13] After the removal of the previously mentioned substances, the samples were washed thoroughly with distilled water and passed through a 300-mesh sieve to separate the sand-sized particles. The mixture of silt and clay-sized particles was kept in tall-form glass bottles. The clay particles were separated by gravity separation with Stokes' law until the upper 10 cm became clear after 8 h.

On the basis of Stokes' law, the collected clay samples were centrifuged at 12,000 rpm for 10 min (equivalent to 17,000 *g*) to fractionate the clay samples in particle sizes of 2000–200 nm (coarse clay) and less than 200 nm (fine clay). The separated fine clays (equivalent diameter < 200 nm) were used for the next step and divided into two equal parts. A portion was treated with 0.2*M* ammonium oxalate, shaken for 2 h in the dark, and then centrifuged[14] to separate the amorphous aluminosilicate materials. All of the clay samples were washed repeatedly to remove excess salts. The concentration of the clay in the suspension was determined separately. So, in this way, a total of six types of clay samples in suspension form were prepared and used for the next experiment.

Preparation of the Nanoclay–Polymer Composites (NCPCs)

A series of samples with different types of clays as fractionated by the aforementioned procedure were used for the synthesis of different NCPCs according to the procedure mentioned by Liang and Liu.[12] Typically, AA (5.76 g) and Am (1.15 g) were dissolved in 10 mL of distilled water and then neutralized with ammonia (neutralization degree = 60%) in a three-necked flask equipped with a condenser, a thermometer, and an N line. The flask was placed on a magnetic stirrer with a heating control. Clay (0.58 g) was then added and dispersed in the partially neutralized monomer solution. Under an N atmosphere, the crosslinker, *N,N′*-methylene bisacrylamide (57.6 mg), was added to the AA/Am/clay mixture solution, and the mixed solution was stirred on the magnetic stirrer at room temperature for 30 min. Then, the temperature was increased slowly to 70°C with vigorous stirring after the radical initiator, ammonium persulfate (80.2 mg), was introduced into the mixed solution. After completion of the polymerization reaction, the resulting product was washed several times with distilled water and then dried at 100°C to a constant weight. Finally, the dried products were milled and screened. All of samples used had a particle size of less than 1 mm in diameter.

Loading of NCPCs with Urea and DAP

The loading of DAP and urea were carried out by the immersion of preweighed dry gels into the aqueous solution of each respective fertilizer for 20 h to reach swelling equilibrium. Thereafter, the swollen gels were dried at 60°C for 6 days. Finally, the dried products were milled and screened.

Analysis of the Nutrient Content of the Fertilizer-Loaded NCPCs

The N and P in the samples were analyzed by the Kjeldhal digestion and colorimetric methods, respectively. For N estimation, 0.5 g sample was added to a 250-mL micro-Kjeldhal flask and digested with 10 mL of concentrated H_2SO_4 in the presence of the digestion mixture. The acid digest was distilled with 40% NaOH, and we titrated the liberated NH_3 absorbed in 4% boric acid with a standard H_2SO_4 (0.1*N*) solution. The content of N was calculated from the volume of H_2SO_4 used for titration. For P estimation, a 0.5-g sample was digested by a diacid mixture ($HNO_3 + HClO_4$) in a conical flask, and the content of P in the digested solution was determined by a colorimetric

Table I. Contents of N and P_2O_5 in the Different Composites

	DAP-loaded		Urea-loaded
Composite	P_2O_5 (%)	N (%)	N (%)
Polymer	19.2	7.8	22.5
Polymer/clay **I(A)**	17.5	6.5	19.4
Polymer/clay **I(B)**	17.8	6.6	19.1
Polymer/clay **II(A)**	16.8	6.3	17.1
Polymer/clay **II(B)**	16.5	6.1	17.8
Polymer/clay **III(A)**	15.4	5.3	17.8
Polymer/clay **III(B)**	14.7	5.4	18.1

method. The concentrations of N and P in the different NCPCs are given in Table I.

Measurement of Equilibrium Water Absorbency

The sample (0.20 g) was immersed in excess distilled water (300 mL) at room temperature for 20 h to reach swelling equilibrium. The swollen sample was then separated from unabsorbed water by filtration through a 100-mesh screen. The water absorbency of the NCPC superabsorbent (Q_{eq}) was calculated with the following equation:

$$Q_{eq} = (m_2 - m_1)/m_1$$

where m_1 and m_2 are the weights of the dry sample and the swollen sample, respectively. Q_{eq} was calculated as grams of water per gram of sample.

Slow-Release Behavior of Nutrients from the NCPCs in Distilled Water

The nutrient-loaded dry NCPC (0.1 g) was added to a tapered bottle, which was filled with 300 mL of distilled water. The contents of N and P in the aqueous solution were determined at 3, 6, 15, 24, and 48 h, and the release curves of N and P for the different NCPCs were obtained.

Characterization of the NCPCs

The NCPCs were characterized by a Fourier transform infrared (FTIR) spectrophotometer (PerkinElmer, Spectrum 100) in the range 4000–450 cm^{-1} with KBr pellets. Power X-ray diffraction (XRD) analyses of the specimens were performed with an X-ray powder diffractometer with a Cu anode (Philips) running at 40 kV and 20 mA, with scanning from 2θs of 3 to 40° at a step angle of 0.1°.

Statistical Analysis

All of the treatment combinations were laid out in a completely randomized design with three replications. An F test was carried out to test the significance of the treatment differences, and the least significant difference (LSD) was computed to test the significance of different treatments at a 5% level of probability by SPSS 11.5 software.

RESULTS

Size and Composition of the Clay Samples Separated from Soils

The clay samples separated from soils were less than 200 nm in diameter. The clays were phyllosilicate, and the ratio of the diameter to the thickness was about 20:1 to 50:1.[12] Therefore, we speculated that the thickness of clay layers was about 4–10 nm. The thickness of the clays was calculated from the width of the XRD peak with software (Phillips automated powder diffractometer), and the data are presented in Table II. We observed that the thickness of clays ranged from 16.3 to 6.9 nm. Figures 1–3 show the transmission electron microscopy (TEM) micrographs of clays **I, II,** and **III,** respectively. Because of their platy morphology, their broader dimensions, that is, length and width, remained parallel to the horizontal and were viewed in the plates. With the aspect ratio (length/thickness) assumed to be 20:1, the approximate thicknesses of clays **I, II,** and **III** were calculated and found to be 8.75, 10, and 5 nm, respectively; these were close to the values obtained from XRD, except for kaolinite. The probable reason might have been that the assumption of the aspect ratio of 20:1 for kaolinite was quite high because due strong hydrogen bonding in the interlayer, the kaolinite particles were thicker than anticipated.

Table II. Thicknesses of the Clay Particles Separated from Soils as Calculated from the Widths of the XRD Peaks of the Mg-Saturated and Glycerol-Solvated Clay Samples and Approximate Thicknesses Obtained from TEM

Clay sample	XRD thickness (nm)	TEM approximate thickness (nm)
Clay **I(A)**	15.8	8.75
Clay **I(B)**	16.3	—
Clay **II(A)**	9.8	10.0
Clay **II(B)**	10.5	—
Clay **III(A)**	6.9	5.0
Clay **III(B)**	7.4	

The typical diffraction patterns of clay samples for Mg-saturated glycerol-solvated specimens are presented in Figure 4. The semiquantitative compositions of the clay samples are presented in Table III. Clay **I** was dominant in kaolinite (80%;

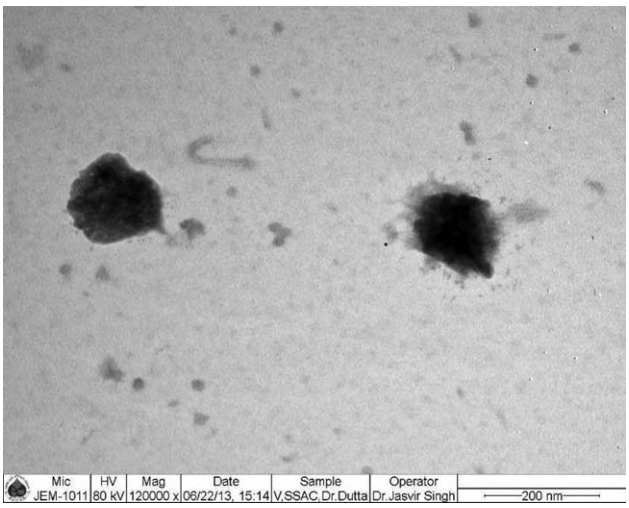

Figure 1. TEM micrographs of clay **I** (kaolinite-dominant clay). The approximate diameter was 175 nm, the assuming aspect ratio was 20:1, and the thickness was 8.75 nm.

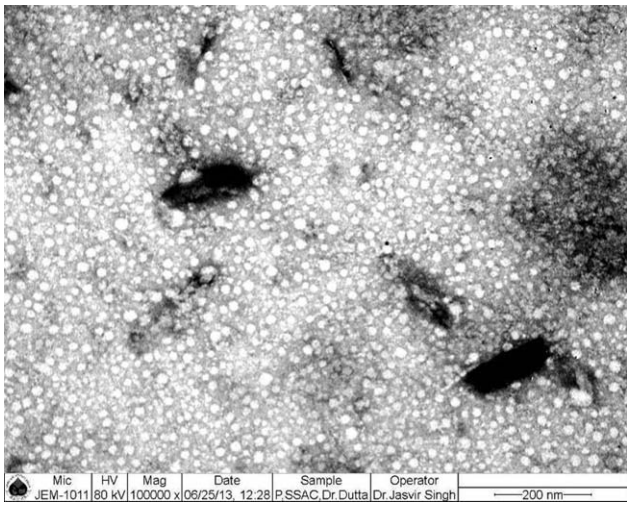

Figure 2. TEM micrographs of clay **II** (mica-dominant clay). The approximate length was 200 nm, the assuming aspect ratio was 20:1, and the approximate thickness was 10 nm.

Table III), as indicated by the presence of a peak around a 2θ of 12.4° [Figure 4(e,f)]. Additionally, it contained small amount (20–21%) of mica, as indicated by the presence of a peak at a 2θ of 8.8° (Figure 4). Clay **II** was dominant in mica (70%), which was indicated by the presence of a peak at a 2θ of 8.8° [Figure 4(c,d)] associated with 13–14% kaolinite (peak at $2\theta = 12.4°$) and 16–17% smectite (peak at $2\theta = 5°$), whereas clay **III** was dominant in smectite (60%), which was indicated by the presence of a peak at a 2θ of 5° [Figure 4(a,b)] associated with 11–12% kaolinite (peak at $2\theta = 12.4°$) and 28% mica–smectite interstratified minerals (peak at $2\theta = 9.5°$). The removal of amorphous aluminosilicates did not significantly affect the compositions of the clay samples.

FTIR Spectra

The FTIR spectra of various clays and their corresponding NCPCs incorporated with 10 wt % clay are shown in Figures 5

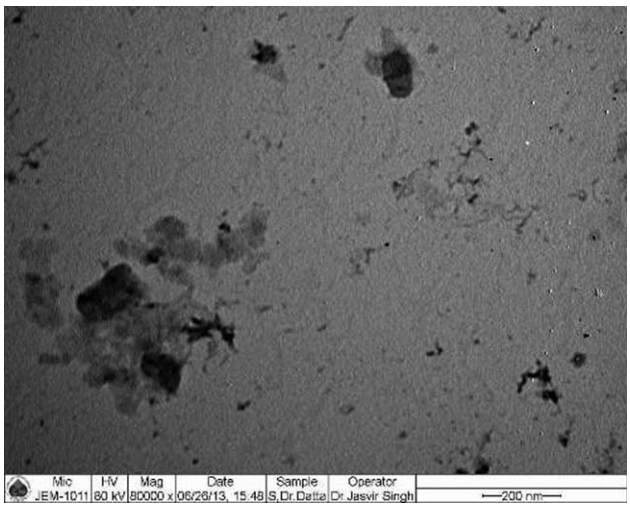

Figure 3. TEM micrographs of clay **III** (smectite-dominant clay). The approximate diameter was 100 nm, the assuming aspect ratio was 20:1, and the thickness was 5 nm.

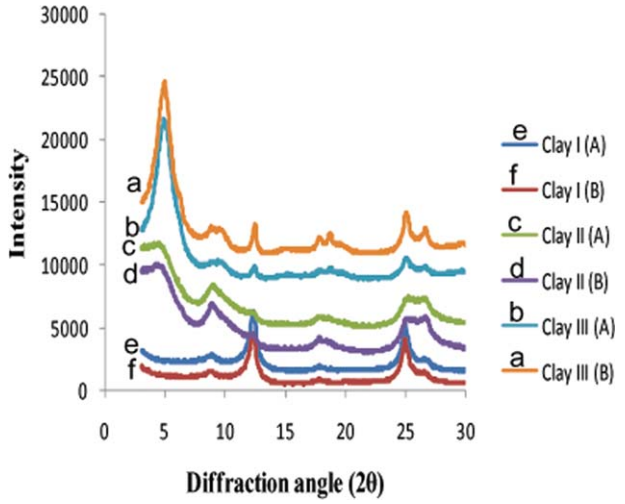

Figure 4. XRD patterns of different nanoclays separated from soils for Mg-saturated and glycerol-solvated samples. [Color figure can be viewed in the online issue, which is available at wileyonlinelibrary.com.]

and 6, respectively. The absorption bands in the range 3400–3700 cm^{-1} were attributed to the stretching of —OH, as shown in Figure 5. The absorption bands at 1637, 1639, 1641, 1638, 1642, and 1639 cm^{-1} in Figure 5(a–f), which were attributed to the —OH bending of H_2O, were found in all of the spectra of the clay samples; this indicated the presence of water in their structures. The absorption bands (Figure 5) in the range 970–450 cm^{-1} were attributed to —OH bending and/or M—O (where M denotes Si or other metal cations existing in the various clays). The vibration bands observed for different clays at 1035, 1035, 1031, 1032, 1028, and 1029 cm^{-1} in Figure 5(a–f) were due to Si—O stretching.

The observed bands at 3439 cm^{-1}, due to the N—H stretching of acryl amide units; 2923 cm^{-1}, due to the C—H stretching of acrylate units; 1690 cm^{-1}, due to the carbonyl moiety of the acryl amide units; and 1167 cm^{-1}, due to the —CO—O^- stretching of acrylate units, are shown in Figure 6(a). The hydrolysis of amide groups was confirmed by the appearance of absorption bands at 1558 cm^{-1} [Figure 6(a,f)], 1564 cm^{-1} [Figure 6(b)], 1572 cm^{-1} [Figure 6(d)], 1562 cm^{-1} [Figure 6(e)], and 1563 cm^{-1} [Figure 6(g)], which were attributed to

Table III. Percentages of Clay Minerals Present in the Clay Samples Separated from Soils

	Types of clay (%)			
Clay sample	Illite/mica	Kaolinite	Smectite	Interstratified (mica + smectite)
Clay **I(A)**	21	79	—	—
Clay **I(B)**	20	80	—	—
Clay **II(A)**	69	14	17	—
Clay **II(B)**	71	13	16	—
Clay **III(A)**	—	12	60	28
Clay **III(B)**	—	11	61	28

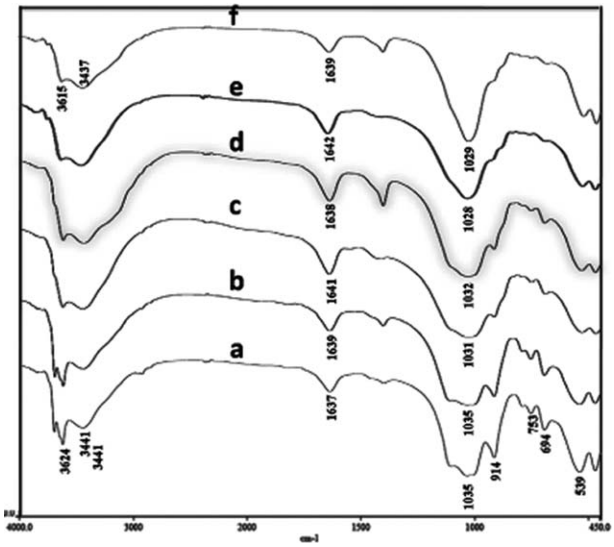

Figure 5. FTIR spectra of the clays: (a) clay **I(A),** (b) clay **I(B),** (c) clay **II(A),** (d) clay **II(B),** (e) clay **III(A),** and (f) clay **III(B).**

—COO^-. The disappearance of the absorption bands of the —OH stretching of various clays in the range 3400–3700 cm^{-1} and the weakening of the absorption bands at about 1030 cm^{-1}, due to Si—O of clays, took place after the incorporation of various clays into the polymer network, as shown in Figure 6(b–g). The absorption band at 1690 cm^{-1}, ascribed to —$CONH_2$ of the polymer, shifted to 1712, 1713, 1708, 1704, and 1717 cm^{-1} in the spectra of polymer/clay **I(A),** polymer/clay **I(B),** polymer/clay **II(A),** polymer/clay **III(A),** and polymer/clay **III(B),** respectively (where **I, II,** and **III** represent clays separated from Alfisol, Inceptisol, and Vertisol, respectively, and **A** and **B** indicate clays with and without amorphous aluminosilicates, respectively); this indicated that the interaction between the clays and polymer network had some influence on the chemical environment of —$CONH_2$ and/or —COO^-. This might have had some influence on the physicochemical properties of the corresponding NCPCs.

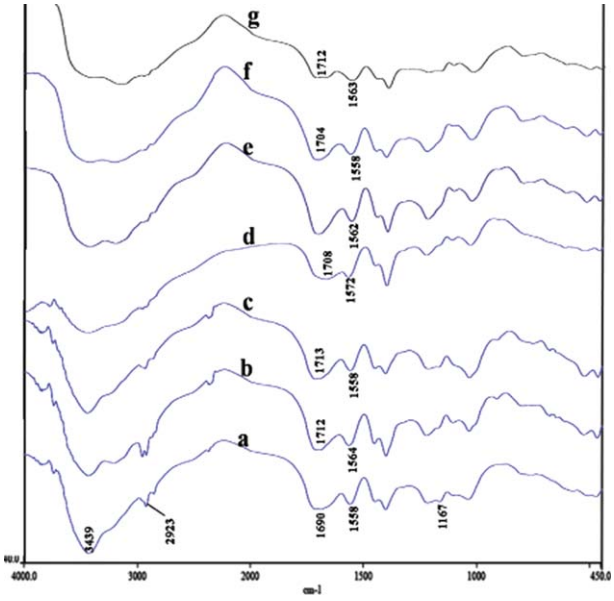

Figure 6. FTIR spectra of the polymer/clays: (a) polymer, (b) polymer/clay **I(A),** (c) polymer/clay **I(B),** (d) polymer/clay **II(A),** (e) polymer/clay **II(B),** (g) polymer/clay **III(A),** and (h) polymer/clay **III(B).** [Color figure can be viewed in the online issue, which is available at wileyonlinelibrary.com.]

XRD Analysis

The reactions between the clay and polymer were also investigated by XRD. The XRD patterns of various clays and their corresponding superabsorbent composites incorporated with 10 wt % clay and a physical mixture of clay with pure polymer (10 wt %) are shown in Figures 7(A,B), 8(A,B), and 9(A,B) for clays **I, II,** and **III,** respectively. As shown in Figure 7(A,B), there were no obvious differences in the position and intensity of the 7.1 Å ($2\theta = 12.4°$) peak for clay **I(A,B),** corresponding polymer/clay **I(A,B)** composites and the polymer/clay **I(A,B)** physical mixture. Similar was the observation for the NCPC incorporated with clay **II(B),** where the typical XRD peak at 9.9 Å ($2\theta = 8.8°$) was also found in the corresponding polymer/clay **II(B)** composite (NCPC) and the polymer/clay **II(B)** physical mixture [Figure 8(B)]. The XRD pattern of clay **III(A,B)** [Figure 9(A,B)] showed a strong peak at $2\theta = 7.0$, which corresponded to a basal spacing of 12.6 Å of the sodium-saturated smectite, which was also found when clay **III(A,B)** was mixed physically with the polymers. After the reaction this peak disappeared in the polymer/clay **III(A,B)** composites.

Influence of the Clay Type on the Equilibrium Water Absorbency

Clay plays an important part in influencing properties of superabsorbent NCPCs because it is the reaction between the clay and the monomer that forms the superabsorbent composite

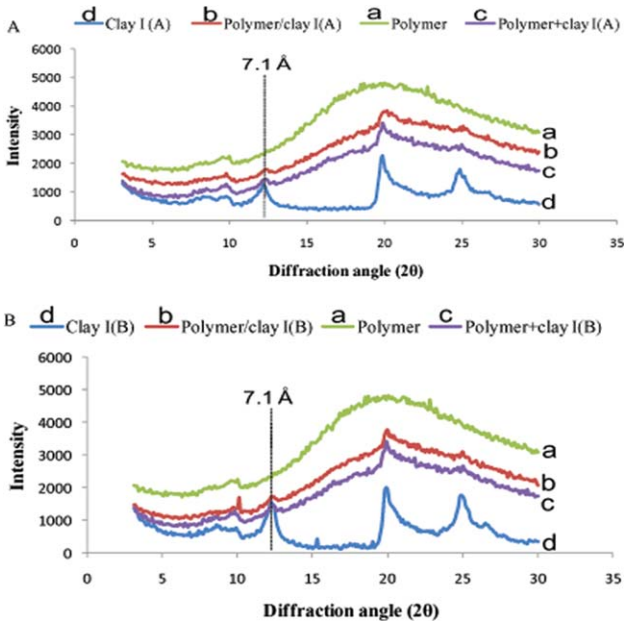

Figure 7. Randomly oriented powder XRD patterns of the clay, polymer/clay composite, polymer, and polymer+clay physical mixture for (A) clay **I(A)** and (B) clay **I(B).** [Color figure can be viewed in the online issue, which is available at wileyonlinelibrary.com.]

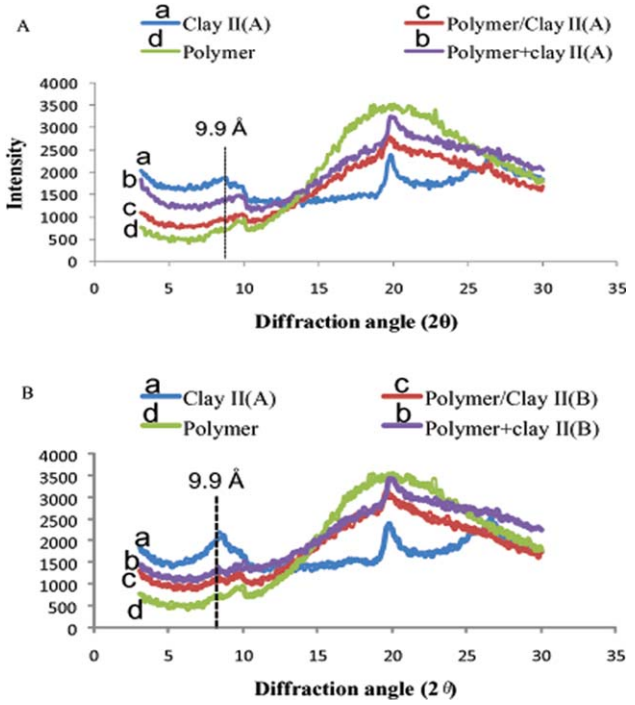

Figure 8. Randomly oriented powder XRD patterns of the clay, polymer/clay composite, polymer, and polymer+clay physical mixture for (1) clay **II(A)** and (2) clay **II(B).** [Color figure can be viewed in the online issue, which is available at wileyonlinelibrary.com.]

polymeric network. In this investigation, six types of clays were introduced into the polymeric network to investigate the effect of the clay type and content on the equilibrium water absorbency of the superabsorbent NCPCs. It is evident from Table IV

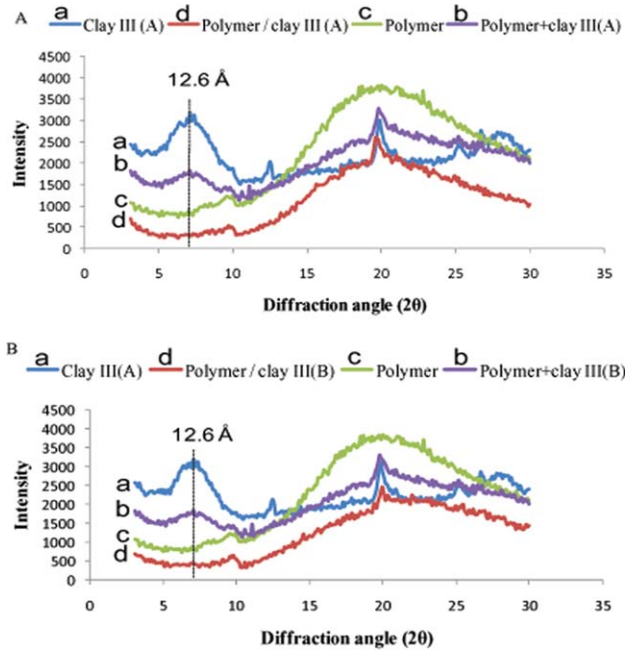

Figure 9. Randomly oriented powder XRD patterns of the clay, polymer/clay composite, polymer, and polymer+clay physical mixture for (A) clay **III(A)** and (B) clay **III(B).** [Color figure can be viewed in the online issue, which is available at wileyonlinelibrary.com.]

Table IV. Variation in the Equilibrium Water Absorbency in Distilled Water for the Polymer/Nanoclay Composites

Composite	Equilibrium water absorbency (g/g)
Polymer	261
Polymer/clay **I(A)**	199
Polymer/clay **I(B)**	204
Polymer/clay **II(A)**	220
Polymer/clay **II(B)**	217
Polymer/clay **III(A)**	174
Polymer/clay **III(B)**	169
LSD ($p < 0.05$)	8

that the incorporation of clays into the polymeric network decreased the equilibrium water absorbency in distilled water regardless of type of clay used.

Also, the equilibrium water absorbency in distilled water for the NCPCs was in the order of Polymer/clay **II(A)** ≈ Polymer/clay **II(B)** > Polymer/clay **I(A)** ≈ Polymer/clay **I(B)** > Polymer/clay **III(A)** ≈ Polymer/clay **III(B).**

Influence of the Clay Type on the Release of N and P in Distilled Water

The slow-release behaviors of P and N from the DAP-loaded composites in distilled water are shown in Figures 10 and 11, respectively, and the N release from the urea-loaded composites is shown in Figure 12. All of the curves were similar in trends of nutrient-release behavior. Initially (up to 15 h), the release rate was high, and then, the rate decreased gradually. The figures also depict a very rapid release from the pure polymer composites (without clay) compared to that from the polymer/clay composites (NCPCs). In case of the pure polymer, the entire amount was released within 15 h of incubation. The

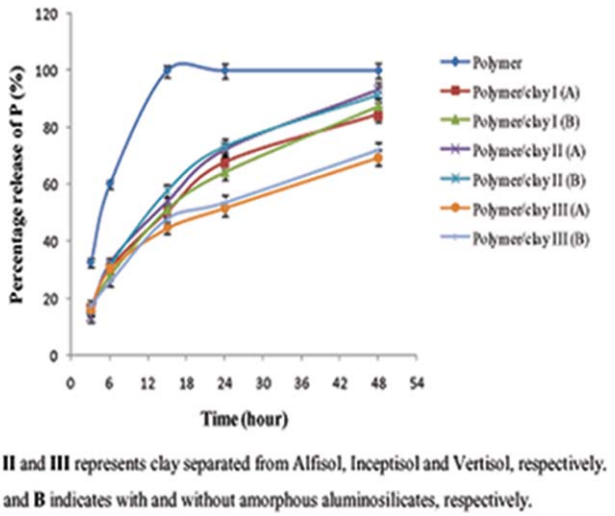

I, II and III represents clay separated from Alfisol, Inceptisol and Vertisol, respectively.
A and B indicates with and without amorphous aluminosilicates, respectively.

Figure 10. Release of P_2O_5 from the DAP-loaded NCPC incorporated with different kinds of clay (10 wt %) in distilled water. [Color figure can be viewed in the online issue, which is available at wileyonlinelibrary.com.]

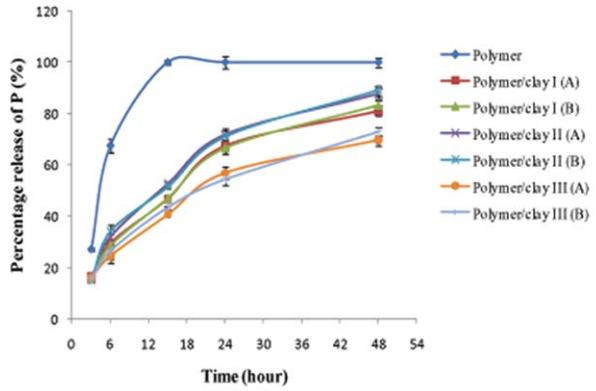

I, II and III represents clay separated from Alfisol, Inceptisol and Vertisol, respectively.

A and B indicates with and without amorphous aluminosilicates, respectively.

Figure 11. Release of N from the DAP-loaded NCPCs incorporated with different kinds of clay (10 wt %) in distilled water. [Color figure can be viewed in the online issue, which is available at wileyonlinelibrary.com.]

presence of amorphous aluminosilicates in the clay did not make any difference in the nutrient-release rate. It was also evident from the figures that in the initial stage (up to 15 h), no significant differences in nutrient release were observed among the polymer/clay composites. Among the various clays used in this study, the incorporation of clay **III** (the smectite-dominated clay) in the polymer matrix was significantly effective in decreasing the amount of nutrient released compared to the that in composites doped with clay **I** (the kaolinite-dominated clay) and clay **II** (the mica-dominated clay). As shown in Figures 10–12, the percentage release of nutrient in all three cases was lower in polymer/clay **I** than in polymer/clay **II** at later stages (24 and 48 h), although the differences were statistically nonsignificant. Among the different NCPCs, the percentage release of nutrients in all three cases at 48 h ranged from around 70% in polymer/clay **III** to 90% in polymer/clay **I** composites.

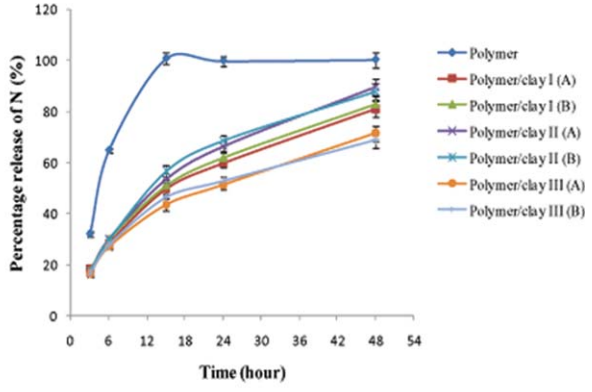

I, II and III represents clay separated from Alfisol, Inceptisol and Vertisol, respectively.

A and B indicates with and without amorphous aluminosilicates, respectively.

Figure 12. Release of N from the urea-loaded NCPCs incorporated with different kinds of clay (10 wt %) in distilled water. [Color figure can be viewed in the online issue, which is available at wileyonlinelibrary.com.]

DISCUSSION

FTIR Spectra

The FTIR spectra showed that the absorption bands of —OH stretching of various clays in the range 3400–3700 cm^{-1} disappeared, and the absorption bands at about 1030 cm^{-1}, ascribed to the Si—O stretching of clays, were weakened after the incorporation of various clays into the polymer network. It was suggested that graft copolymerization between the —OH groups on kaolin and the monomers took place during the polymerization reaction.[12] Lin et al.[10] reported that AA could graft onto mica and form a poly(acrylic acid)/mica superabsorbent composite. The —OH group of kaolinite could react with acrylamide, and kaolinite particles could chemically bond with the polymer chains to form a starch-*graft*-acryl amide/kaolinite composite.[3] Thus, the disappeared and weakened absorption bands may have been due to the same reason, and the clays reacted with monomer unit during the polymerization process. The absorption band at 1690 cm^{-1}, ascribed to the —$CONH_2$ of the pure polymer, shifted to 1712, 1713, 1708,1704, and 1717 cm^{-1} in the spectra of polymer/clay **I(A),** polymer/clay **I(B),** polymer/clay **II(A),** polymer/clay **III(A),** and polymer/clay **III(B),** respectively; this indicated that the interaction between the clays and polymer had some influence on the chemical environment of —$CONH_2$ and/or —COO^- and might have had some influence on the physicochemical properties of the corresponding superabsorbent composites.

XRD Analysis

The XRD pattern showed no obvious differences in the typical diffraction peaks (7.1 Å) of clay **I** (kaolinite dominated) and 9.9 Å of clay **II** (mica dominated) and their corresponding polymer/clay composites. This suggested that the reaction between the polymer and clays **I** and **II** occurred on the surface of the various clay particles without intercalating into the stacked silicate galleries. This was attributed to the structure and reactivity differences of the clays. For the kaolinite-dominated clay (clay **I**), the polymer chains could not be intercalated into the silicate galleries because there were no permanent negative charges on the silicate galleries and the intensive hydrogen-bond effect between the layers. This result conformed with those of a previous study.[16] After clay **III** (the smectite-dominated clay) was incorporated into the polymeric network, the typical diffraction peak of the smectite clay disappeared; this indicated the intercalation of the polymer into the stacked silicate galleries of the clay and the exfoliation of the clay.

Effect of the Clay Type on the Water Absorbency and Nutrient Release

The results show that the incorporation of clays into the polymeric network decreased the equilibrium water absorbency and nutrient-release rate in distilled water, regardless of the type of clay used. The reasons for the decreased water absorbency and nutrient-release rate might be interpreted as follows: the introduction of clay particles into the polymeric network increased the crosslinking density of polymer, and then, the elasticity of the polymer chains decreased. Large crosslinking density meant not enough space for water molecules to enter the network; this resulted in the lower equilibrium water absorbency. This results

were in conformity with the findings of some previous studies;[12,16] similarly, the incorporation of nanoclays into polymeric network decreased the mesh size of the polymer/clay composites (NCPCs). This enhanced the barriers of nutrient diffusion, so the release of nutrients slowed down. We also observed that equilibrium water absorbency in distilled water for the polymer/clay composites was in the order Polymer/clay **II** > Polymer/clay **I** > Polymer/clay **III,** and the trend of nutrient-release percentages also followed same order. However, no significant differences in the nutrient-release rate were observed between polymer/clay **I** and polymer/clay **II.** This might have been due to the hydration and distention differences in these clays as reported previously by Wu et al.[6] in the starch-*graft*-acryl amide/clay system and Zhang and Wang[15] in polyacrylamide/clay composites for water absorbency. The higher hydration and distention might have increased the interaction between the polymeric network and clay, which increased the crosslinking density of the obtained superabsorbent composites and then decreased the equilibrium water absorbency and nutrient-release rate. For example, clay **III** (the smectite-dominated clay) had the highest hydration and distention among the selected clays; this resulted in more crosslinking in the composite, which in turn, resulted in the lowest equilibrium water absorbency and nutrient-release rate of the corresponding NCPC.

CONCLUSIONS

In case of the NCPC incorporated with clay **I** (the kaolinite-dominated clay) and clay **II** (the mica-dominated clay), the reaction occurred on the surface of the clays. However, the polymer layer penetrated into silicate layers, and the clay was exfoliated when clay **III** (the smectite-dominated clay) was introduced. The equilibrium water absorbency and nutrient-release rate decreased with the incorporation of clay into the polymer matrix because of the increase in crosslinking points and the decrease in the mesh size of the NCPCs as compared to those in the pure polymer. This crosslinking was maximum in case of the smectite clay. So, the study suggested that the smectite type of clay should be selected to prepare NCPCs to obtain better slow-release properties. No effect was found with the presence of amorphous aluminosilicate in the clay.

REFERENCES

1. Ladha, J. K.; Pathak, H.; Krupnik, T. J.; Six, J.; Van Kessel, C. *Adv. Agronomy* **2005**, *87*, 85.
2. Malhi, S. S.; Haderlein, L. K.; Pauly, D. G.; Johnston, A. M. *Better Crops* **2002**, *86*, 8.
3. Al-Zahrani, S. M. *Ind. Eng. Chem. Res.* **2000**, *39*, 367.
4. Anupama, K. R.; Jat, M. L.; Parmar, B. S. *Acta Hort.* **2007**, *742*, 43.
5. Mohan, Y. M.; Murthy, P. S. K.; Raju, K. M. *React. Funct. Polym.* **2005**, *63*, 11.
6. Wu, J.; Wei, Y.; Lin, J.; Lin, S. *Polymer* **2003**, *44*, 6513.
7. Lee, W. F.; Yang, L. G. *Polym. Adv. Technol.* **2004**, *92*, 3422.
8. Kabiri, K.; Zohuriaan-Mehr, M. *J. Macromol. Mater. Eng.* **2004**, *289*, 653.
9. Li, A.; Wang, A.; Chen, J. *J. Appl. Polym. Sci.* **2004**, *94*, 1869.
10. Lin, L.; Wu, J. H.; Yang, Z.; Pu, M. L. *Macromol. Rapid Commun.* **2001**, *22*, 422.
11. Wu, J. H.; Lin, J. M.; Zhou, M.; Wei, C. R. *Macromol. Rapid Commun.* **2000**, *22*, 1032.
12. Liang, R.; Liu, M. *J. Appl. Polym. Sci.* **2007**, *106*, 3007.
13. Jackson, M. L. Soil Chemical Analysis—Advanced Course: A Manual of Methods Useful for Instruction and Research in Soil Chemistry, Physical Chemistry of Soils, Soil Fertility, and Soil Genesis, 2nd ed.; Jackson: Madison, WI, **1969**; Chapters 2 and 3, p 27.
14. Fey, M. V.; Le Roux, *J. Clays Clay Miner.* **1977**, *25*, 285.
15. Zhang, J.; Wang, A. *React. Funct. Polym.* **2007**, *67*, 737.